

Bromotryptamine and Bromotyramine Derivatives from the Tropical Southwestern Pacific Sponge *Narrabeena nigra*

Maria Miguel-Gordo, Sandra Gegunde, Kevin Calabro, Laurence Jennings,
Amparo Alfonso, Grégory Genta-Jouve, Jean Vacelet, Luis Botana, Olivier
Thomas

► **To cite this version:**

Maria Miguel-Gordo, Sandra Gegunde, Kevin Calabro, Laurence Jennings, Amparo Alfonso, et al..
Bromotryptamine and Bromotyramine Derivatives from the Tropical Southwestern Pacific Sponge
Narrabeena nigra. *Marine drugs*, MDPI, 2019, 17 (6), pp.1-18/319. 10.3390/md17060319 . hal-
02146552

HAL Id: hal-02146552

<https://hal-amu.archives-ouvertes.fr/hal-02146552>

Submitted on 4 Jun 2019








HAL is a multi-disciplinary open access archive for the deposit and dissemination of scientific research documents, whether they are published or not. The documents may come from teaching and research institutions in France or abroad, or from public or private research centers.

L'archive ouverte pluridisciplinaire **HAL**, est destinée au dépôt et à la diffusion de documents scientifiques de niveau recherche, publiés ou non, émanant des établissements d'enseignement et de recherche français ou étrangers, des laboratoires publics ou privés.



Article

Bromotryptamine and Bromotyramine Derivatives from the Tropical Southwestern Pacific Sponge *Narrabeena nigra*

Maria Miguel-Gordo ¹, Sandra Gegunde ², Kevin Calabro ¹, Laurence K. Jennings ¹, Amparo Alfonso ², Grégory Genta-Jouve ^{3,4}, Jean Vacelet ⁵, Luis M. Botana ^{2,*} and Olivier P. Thomas ^{1,*}

¹ Marine Biodiscovery, School of Chemistry and Ryan Institute, National University of Ireland Galway (NUI Galway), University Road, H91 TK33 Galway, Ireland; m.miguelgordo1@nuigalway.ie (M.M.-G.); kevin.calabro@nuigalway.ie (K.C.); laurence.jennings@nuigalway.ie (L.K.J.)

² Departamento de Farmacología, Facultad de Veterinaria, Universidade de Santiago de Compostela, 27002 Lugo, Spain; sandra.gegunde@rai.usc.es (S.G.); amparo.alfonso@usc.es (A.A.)

³ Laboratoire de Chimie-Toxicologie Analytique et Cellulaire (C-TAC) UMR CNRS 8038 CiTCoM Université Paris-Descartes, 4, avenue de l'Observatoire, 75006 Paris, France; gregory.genta-jouve@parisdescartes.fr

⁴ Muséum National d'Histoire Naturelle, Unité Molécules de Communication et Adaptation des Micro-organismes (UMR 7245), Sorbonne Universités, CNRS, 75005 Paris, France

⁵ Aix Marseille Université, CNRS, IRD, IMBE UMR 7263, Avignon Université, Institut Méditerranéen de Biodiversité et d'Écologie marine et continentale, Station Marine d'Endoume, Chemin de la Batterie des Lions, 13007 Marseille, France; jean.vacelet@imbe.fr

* Correspondence: luis.botana@usc.es (L.M.B.); olivier.thomas@nuigalway.ie (O.P.T.); Tel.: +34-9828-22233 (L.M.B.); +353-9149-3563 (O.P.T.)

Received: 28 April 2019; Accepted: 28 May 2019; Published: 30 May 2019



Abstract: So far, the Futuna Islands located in the Central Indo-Pacific Ocean have not been inventoried for their diversity in marine sponges and associated chemical diversity. As part of the Tara Pacific expedition, the first chemical investigation of the sponge *Narrabeena nigra* collected around the Futuna Islands yielded 18 brominated alkaloids: seven new bromotryptamine derivatives **1–7** and one new bromotyramine derivative **8** together with 10 known metabolites of both families **9–18**. Their structures were deduced from extensive analyses of nuclear magnetic resonance (NMR) and high-resolution mass spectrometry (HRMS) data. *In silico* metabolite anticipation using the online tool MetWork revealed the presence of a key and minor biosynthetic intermediates. These 18 compounds showed almost no cytotoxic effect up to 10 μ M on human neuroblastoma SH-SY5Y and microglia BV2 cells, and some of them exhibited an interesting neuroprotective activity by reducing oxidative damage.

Keywords: Futuna; Porifera; *Narrabeena*; coral reefs; aromatic alkaloids; Bromotryptamine; Bromotyramine; neuroprotective agents

1. Introduction

Bioprospection represents the first step of the marine biodiscovery process, followed by the description of bioactive molecules, which can find applications especially in human health and the pharmaceutical sector. The Indo-Pacific Ocean is considered a key geographical area for marine biodiscovery, not only because of its luxuriant marine biodiversity, but also because marine invertebrates of remote islands usually present a high rate of endemism, then leading to a potential chemical novelty. Importantly, inventories of the marine biodiversity around isolated islands also contribute to a global

understanding of our oceans using an integrative approach composed of taxonomy, chemistry, ecology, biology, biochemistry, and microbiology [1–3]. The Tara Pacific expedition (2016–2018) explored the Pacific Ocean with the main scientific objective to conduct a comprehensive description of the marine biodiversity present in endangered coral reefs, from genes to ecosystem. In this context, an inventory of marine sponges was achieved in some locations for the first time, with the second objective to describe their associated chemical diversity [4]. The islands of Wallis and Futuna are located in the biodiversity-rich Tropical Southwestern Pacific, and only little information has been given about the biodiversity of marine invertebrates in this territory, mostly around the island of Wallis [5,6]. To the best of our knowledge, no detailed inventory of littoral sponges has been reported so far from the Futuna Islands composed of the two islands: Futuna and Alofi [7–9].

Following preliminary chemical profiling of the fractions obtained from sponges collected in this area, the sponge *Narrabeena nigra* Kim and Sim, 2010, first described in Korea [10] was selected for a thorough chemical investigation due to the presence of a high diversity of brominated alkaloids. Even though no natural products have been reported for species of this genus, other species of the Thorectidae family such as *Smenospongia* sp. and *Hyrtios* sp. are known to produce metabolites of this family with cytotoxic [11–13], anti-inflammatory, antioxidant [14], and antidepressant activities [15]. We describe herein the isolation and structure elucidation of seven new bromotryptamine metabolites 1–7 and a new bromotyramine derivative 8 (Figure 1), along with 10 known brominated analogues: 5,6-dibromo-*N,N*-dimethyltryptamine (9) [16,17], 5,6-dibromo-*N*-methyltryptamine (10) [18], 5,6-dibromotryptamine (11) [18], 6-bromo-*N*-methyltryptamine (12) [19], 6-bromotryptamine (13) [20,21], 6-bromokynuramine (14) [22], 7-bromoquinolin-4(1*H*)-one (15) [22], 3,5-dibromo-4-methoxytyramine (16) [23], 3-bromo-4-methoxy-*N,N,N*-trimethyltyrosine (17) [24], and 3-bromo-4-methoxytyramine (18), isolated for the first time as a natural product but widely used as a reactant in synthesis [23]. The biological activity of these alkaloids was assessed on two cellular models associated with neuroinflammation [25].

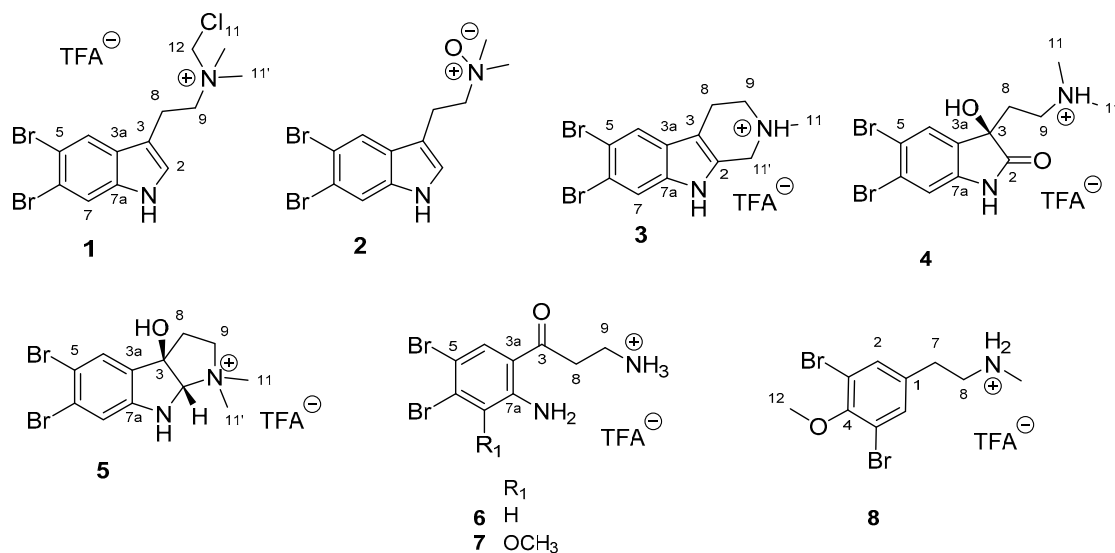


Figure 1. Chemical structures of seven new bromotryptamine and one new bromotyramine derivatives isolated from the sponge *Narrabeena nigra*.

2. Results and Discussion

2.1. Isolation and Structure Elucidation

The freeze-dried sponge sample (66.8 g) was extracted with MeOH/CH₂Cl₂ (1:1) under sonication three times. The extract was then fractionated by reversed phase (RP)-C18 vacuum liquid chromatography (VLC) with solvents of decreasing polarity: H₂O, H₂O/MeOH (1:1), MeOH,

MeOH/CH₂Cl₂ (1:1), and CH₂Cl₂. Compounds of the H₂O/MeOH, MeOH, and MeOH/CH₂Cl₂ fractions were then purified by repeated preparative, semi-preparative, and analytical RP-HPLC, leading to the isolation of 18 pure metabolites, including the new tryptamine alkaloids **1–7** and the new tyramine derivative **8**. As the known 5,6-dibromo-*N,N*-dimethyltryptamine (**9**) and 3,5-dibromo-4-methoxytyramine (**16**) were found to be the major metabolites of the extract, the structures of the new metabolites were mainly deduced by comparison of their nuclear magnetic resonance (NMR) and high resolution mass spectrometry (HRMS) spectra with those of both **9** and **16**.

Compound **1** was isolated as a yellow amorphous solid, and its HRMS spectrum revealed the molecular formula C₁₃H₁₆Br₂ClN₂ calculated from the ion at *m/z* 392.9366 [M]⁺ and an isotopic pattern characteristic of the presence of two bromine and one chlorine atoms. The ¹H NMR spectrum of **1** evidenced the presence of a 3, 5, 6-trisubstituted indole ring system with characteristic singlets at δ_H 7.30 (s, H-2), 7.98 (s, H-4), and 7.74 (s, H-7) (Table 1). Two additional signals of the AA'XX' system at δ_H 3.27 (H-8) and the deshielded signal at δ_H 3.73 (H-9) were reminiscent of a quaternary tryptammonium ion. The signal at δ_H 3.33 (s, H₃-11 and H₃-11') first revealed two equivalent methyls placed on the terminal amine. When comparing with known derivatives of this family, the NMR data of **1** were similar to those of the known 5,6-dibromo-*N,N*-dimethyltryptamine (**9**), with the presence of an additional deshielded signal of a methylene group at δ_H 5.39 (s, H₂-12) and δ_C 68.2 (C-12) (Tables 1 and 2) [17]. These unusual signals perfectly matched with the signals corresponding to the rare *N*-(chloromethyl) substituent, as exemplified by NMR data of plant *N*-(chloromethyl)tryptamine derivatives [26]. The structure was confirmed first using the key H-12/C-9, C-11 and C-11' heteronuclear multiple bond correlation (HMBC) correlations and then the fragments at *m/z* 344.9466 and 301.8995 in the HRMS/MS spectrum of **1**, indicative of the loss of a *N*-chloromethyl and chloromethyl dimethylamine moieties, respectively. Therefore, **1** was identified as the trifluoroacetate (TFA) salt of 5,6-dibromo-*N*-chloromethyl-*N,N*-dimethyltryptammonium. *N*-chloromethyl derivatives have been commonly found as artefact products of the alkylation of tertiary amines by dichloromethane [27]. As we were unable to find a trace of **1** by ultra-high performance liquid chromatography (UHPLC)-HRMS/MS analysis of the ethanolic extract prepared from the same sponge specimen, we could conclude that **1** is produced during the extraction process.

Table 1. ¹H NMR data: δ_H in ppm, mult. (*J* in Hz), in CD₃OD for **1–7** and **9**.

Position	9 ^a	1 ^b	2 ^b	3 ^a	4 ^b	5 ^a	6 ^a	7 ^a
2	7.26	7.30, s	7.26, s	-	-	5.18, s	-	-
4	7.93, s	7.98, s	7.99, s	7.85, s	7.73, s	7.62, s	7.98, s	7.87, s
7	7.70, s	7.74, s	7.72, s	7.72, s	7.25, s	7.14, s	7.19, s	-
8a	3.14, t	3.27, AA'XX'	-	3.11, t	2.43, dt (15.0, 7.5)	2.73, m	3.35, t	3.37, t
8b	(7.5)	(<i>J</i> _{AX} 12 <i>J</i> _{AX'} 5)	3.33 ^c	(6.0)	2.06, ddd (15.0, 7.5, 5.0)	2.57, m	(6.0)	(6.0)
9a	3.39, t	3.73, AA'XX'	-	3.83, m	3.58, dt (15.0, 7.5)	3.68, m	3.29, t	-
9b	(7.5)	(<i>J</i> _{AX} 12 <i>J</i> _{AX'} 5)	3.72, m	3.53, m	3.37 ^c	3.26, m	(6.0)	3.32 ^c
11	-	-	-	3.12, s	-	3.25, s	-	-
11'	2.93, s	3.33, s	3.42, s	4.62, m	2.94, s	-	-	-
12	-	5.39, s	-	4.45, m	-	3.01, s	-	-
CH₃-O	-	-	-	-	-	-	-	3.81, s

^a 500MHz ^b 600MHz ^c Overlap with solvent signal.

The molecular formula of **2**, isolated as a colorless amorphous solid, was deduced as C₁₂H₁₄Br₂N₂O from the molecular ion at *m/z* 360.9557 [M + H]⁺, showing an isotopic pattern of two bromine atoms. While the ¹H NMR and ¹³C NMR spectra were very similar to those of **9**, the signals corresponding to the H₂-9 methylene and the two *N*-methyls were strongly deshielded. Because **2** showed a molecular mass 16 amu higher than **9**, it was proposed to be the *N*-oxide analogue of **9**. This assumption was confirmed by the presence of a fragment at *m/z* 301.9008 in HRMS/MS, revealing the loss of the *N,N*-dimethylamine-*N*-oxide fragment. Thus, **2** was established as 5,6-dibromo-*N,N*-dimethyltryptamine-*N*-oxide.

Table 2. ^{13}C NMR data (150 MHz), δ_{C} in ppm, type, in CD_3OD for **1–7** and **9**.

Position	9	1	2	3	4	5	6	7
2	126.8, CH	125.6, CH	126.7, CH	128.8, C	180.3, C	100.7, CH		
3	109.7, C	107.4, C	110.1, C	106.3, C	75.3, C	88.4, C	198.9, C	199.1, C
3a	129.1, C	127.6, C	129.3, C	128.1, C	134.1, C	134.1, C	118.2, C	118.6, C
4	123.5, CH	122.1, CH	123.7, CH	123.7, CH	130.1, CH	129.8, CH	136.1, CH	131.1, CH
5	117.5, C	116.3, C	117.3, C	118.2, C	118.3, C	115.5, C	108.7, C	108.8, C
6	115.0, C	113.8, C	114.9, C	115.6, C	126.5, C	127.0, C	132.4, C	126.6, C
7	117.3, CH	116.1, CH	117.3, CH	117.3, CH	116.6, CH	116.3, CH	122.8, CH	147.7, C
7a	137.8, CH	136.4, CH	137.8, C	138.0, C	142.9, C	149.7, C	152.4, C	146.1, C
8	21.5, CH_2	18.0, CH_2	20.0, CH_2	19.5, CH_2	32.6, CH_2	39.0, CH_2	36.6, CH_2	36.8, CH_2
9	58.8, CH_2	62.7, CH_2	70.9, CH_2	53.6, CH_2	54.4, CH_2	62.2, CH_2	36.0, CH_2	36.0, CH_2
11				43.1, CH_3		46.9, CH_3		
11'	43.5, CH_3	48.5, CH_3	57.6, CH_3	51.8, CH_2	43.8, CH_3	49.9, CH_3		
12		68.2, CH_2						
$\text{CH}_3\text{-O}$								59.9, CH_3

Compound **3** was isolated as a colorless amorphous solid, showing a molecular ion at m/z 342.9433 $[\text{M} + \text{H}]^+$, corresponding to the molecular formula $\text{C}_{12}\text{H}_{12}\text{Br}_2\text{N}_2$. The aromatic region of the ^1H NMR spectrum was consistent with a 5,6-dibromosubstituted indole. However, the signal corresponding to H-2 was missing when compared to **1** and **2**, indicating this position was substituted. While only one nitrogenated methyl was evidenced in **3** at δ_{H} 3.12 (s, $\text{H}_3\text{-11}$), other broad signals appeared in the ^1H NMR at δ_{H} 4.62, 4.45 ($\text{H}_2\text{-11}'$), 3.83, 3.53 ($\text{H}_2\text{-9}$) in addition to the signal of the methylene protons at δ_{H} 3.11 (t, $J = 6$ Hz, $\text{H}_2\text{-8}$). The correlation spectroscopy (COSY) and heteronuclear single quantum coherence (HSQC) spectra were not helpful to solve the structure due to the broadening of the signals of the two first methylene groups. Gratifyingly, key H-11/C-11' and C-9 HMBC correlations were highly informative to place the two methylene groups next to the tertiary amine. The only possibility to comply with the molecular formula and the substitution at C-2 was therefore to envisage the presence of a *N*-methyl substituted tetrahydro- β -carboline. Broadening of the signals at C-9 and C-11' is easily explained as the protonated tertiary amine becomes chiral in the acidic medium used during the purification process [28]. This is the first report of the 6,7-dibromo-2-methyltetrahydro- β -carboline.

Compound **4** was obtained as a yellow amorphous solid, and its molecular formula $\text{C}_{12}\text{H}_{14}\text{Br}_2\text{N}_2\text{O}_2$ was deduced from the protonated adduct at m/z 376.9503 $[\text{M} + \text{H}]^+$ in its HRMS spectrum. The ^1H NMR spectrum again revealed the presence of a 5,6-dibromosubstituted indole ring system but, as in **3**, the signal corresponding to H-2 was absent in **4**. The ^{13}C NMR spectrum revealed the presence of two new non-protonated carbons: A carbonyl group at δ_{C} 180.3 (qC, C-2) and an oxygenated sp^3 carbon at δ_{C} 75.3 (qC, C-3). A key H-4/C-3 HMBC correlation placed the non-protonated oxygenated carbon at C-3, while a unique H-8a/C-2 HMBC correlation was consistent with the carbonyl group at C-2. The C-2/C-3 bond of the indole ring of **4** was therefore oxidized into a 3-hydroxyindolin-2-one, and the chemical shifts of the carbons at both positions were in accordance with those of analogues in this series [29]. Two non-equivalent methylenes coupled in the ABMX system at δ_{H} 2.43 (dt, $J = 15.0, 7.5$ Hz, H-8a), 2.06 (ddd, $J = 15.0, 7.5, 5.0$ Hz, H-8b), and 3.58 (dt, $J = 15.0, 7.5$ Hz, H-9a), 3.37 (m, H-9b), therefore confirming the presence of a chiral center at C-3. The absolute configuration at C-3 was assessed by comparison between the experimental and calculated electronic circular dichroism (ECD) spectra. The ECD spectra of both enantiomers of **4** were calculated using time-dependent density functional theory (TDDFT) at the B3LYP/6-311+G(d,p)//B3LYP/6-31G(d) level of theory. Not surprisingly, the calculated ECD spectrum of the 3*R* enantiomer matched the experimental spectrum of **4**, as this configuration is also found for most of the natural products containing a 3-hydroxyindolin-2-one (Figure 2). Finally, **4** was named narrabeenamaine A.

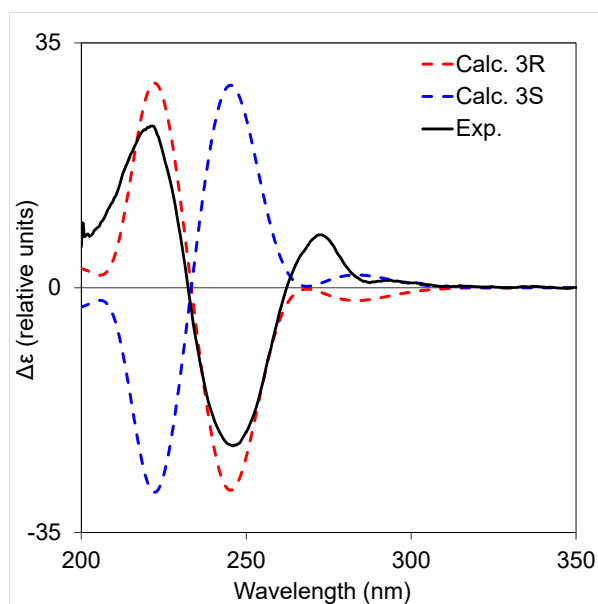


Figure 2. Comparison between the calculated and experimental electronic circular dichroism (ECD) spectra of both enantiomers of **4**.

Compound **5** was isolated as a yellow amorphous solid, and its molecular formula $C_{12}H_{15}Br_2N_2O$ was deduced from the ion peak of the HRMS spectrum at m/z 360.9551 $[M]^+$. Like **3** and **4**, the 5,6-dibromosubstituted benzene ring system was deduced from the two aromatic proton singlets at δ_H 7.62 (s, H-4) and 7.14 (s, H-7), but the signal corresponding to H-2 was again absent. The presence of a non-protonated oxygenated carbon signal at δ_C 88.4 (qC, C-3), together with the key H-4/C-3 HMBC correlation, suggested the presence of a hydroxyl group at C-3. Since no carbonyl signal was observed in the ^{13}C NMR spectrum, a different substitution pattern at C-2 was deduced for **5** when compared to **4**. The 1H and ^{13}C NMR spectra of **5** revealed the presence of one methine group with the proton and carbon signals at δ_H 5.18 (s, H-2) and δ_C 100.7 (CH, C-2) and two non-equivalent *N*-methyl groups at δ_H 3.25 (s, H₃-11) and 3.01 (s, H₃-11'). Moreover, H-2/C3, C-7a, C-9, and H-11/C-2, C-9 HMBC correlations revealed the presence of a third ring system containing the amina functional group of a hexahydropyrrolo[2,3-*b*]indole skeleton (Figure 3). Comparison of the NMR data of **5** with those of other natural products in this series confirmed our assumption and **5** was named narrabeenamine B [30].

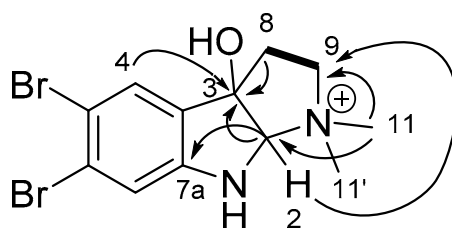


Figure 3. Key correlation spectroscopy COSY (bold) and heteronuclear multiple bond correlation HMBC (arrows from H to C) for narrabeenamine B (**5**).

The absolute configurations at the C-2 and C-3 chiral centers were assessed by comparison between the experimental and calculated ECD spectra of the 4 possible diastereoisomers. Indeed, the NOESY spectrum did not allow the assignment of the relative configurations even if the spectrum was run in DMSO- d_6 . The ECD spectra of the four possible configurations of **5** were therefore calculated using TDDFT at the B3LYP/6-311+G(d,p)//B3LYP/6-31G(d) level of theory. As in **4**, the negative Cotton effect at 250 nm suggested a 3*R* configuration. Comparison between the calculated ECD spectra of both (2*S*, 3*R*) and (2*R*, 3*R*) epimers and the experimental ECD spectrum of **5** evidenced the presence of an additional key Cotton effect of a $\pi \rightarrow \pi^*$ transition at approximately 290 nm, which is associated with the configuration at C-2. The negative Cotton effect observed at 310 nm in the experimental spectrum of **5** was in accordance with the (2*S*, 3*R*) relative configurations (Figure 4).

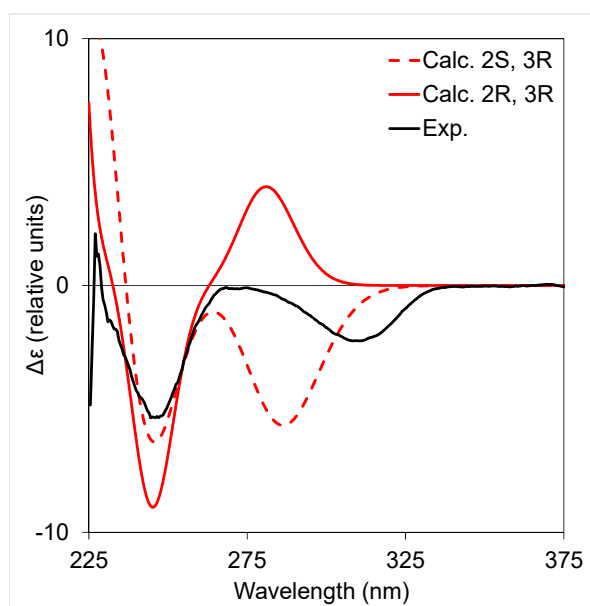


Figure 4. Comparison of the calculated and experimental ECD spectra of the two epimers of **5** at C-2.

The molecular formula $C_9H_{10}Br_2N_2O$ of **6**, a yellow amorphous solid, was deduced from the ion at m/z 320.9239 $[M + H]^+$ of its HRMS spectrum. The 1H NMR spectrum of **6** exhibited two aromatic proton signals at δ_H 7.98 (s, H-4) and 7.19 (s, H-7), suggesting again the presence of the 5,6-dibromobenzene ring of the indole ring system and two coupled methylene protons. However, the signals corresponding to H-2 and the methyls were absent, while the presence of a ketone was evidenced by the signal at δ_C 198.9 (qC, C-3) in the ^{13}C NMR spectrum. The key H-4/C3, C-3a, C-5, C-6, C-7a HMBC correlations placed the ketone at the *ortho* position of the aromatic amino group (C-3 respecting the previous numbering), and the ethylene moiety connected the ketone to another primary amine. Cleavage of the C-2/C-3 bond and loss of the resulting formamide were therefore proposed in order to match the molecular formula. This skeleton is also found in natural products, as exemplified in 5,6-dibromokynuramine [22].

Compound **7** was obtained as a yellow amorphous solid and showed a main ion at m/z 350.9344 $[M + H]^+$ in its HRMS spectrum, leading to the molecular formula $C_{10}H_{12}Br_2N_2O_2$. The 1H NMR and HSQC spectra revealed the presence of one aromatic proton signal at δ_H 7.87 (s, H-4) and a signal of a methoxy group at δ_H 3.81 (s, \underline{CH}_3O-), while the other signals were very similar to those of **6**. The location of the methoxy group at C-7 of the aromatic ring was inferred from the key $\underline{CH}_3-O/C-7$ HMBC correlation. Therefore, **7** is the methoxylated analogue of **6** at C-7.

Compound **8** was isolated as a colorless amorphous solid with a molecular formula $C_{10}H_{13}Br_2NO$ as deduced from the $[M + H]^+$ ion at m/z 321.9447. The 1H NMR spectrum of **8** did not correspond to an indole derivative, as the only aromatic signal at δ_H 7.55 (s, H_{2-6}) was integrated for two protons. The symmetry for the aromatic ring of a dibrominated compound quickly led us to propose a tyramine derivative for **8**. The analogy with the known 3,5-dibromo-4-methoxytyramine (**16**) was evident, and the additional nitrogenated methyl observed at δ_H 2.72 (s, CH_3NH-) revealed that **8** is indeed the new *N*-methyl analogue of **16**.

2.2. Biological Assays

Since human neuroblastoma SH-SY5Y and microglia BV2 cells are commonly used for biological studies of neuroinflammation and neuroprotection [31,32], all isolated brominated alkaloids were then tested in these two cellular models. First, the effects of these compounds on cell viability were determined using the 3-(4,5-dimethylthiazol-2-yl)-2,5-diphenyltetrazolium bromide (MTT) assay. Cells were treated with different concentrations of compounds (0.001, 0.01, 0.1, 1, and 10 μ M) for 24 h. None of the tested compounds induced cytotoxic effects on BV2 cells at any concentrations tested. Furthermore, among the 18 compounds tested on SH-SY5Y neuroblastoma cells, only **3** at 10 μ M reduced cell viability up to 60% ($p < 0.05$) versus control cells. To evaluate the neuroprotective effects of these compounds, *tert*-butyl hydroperoxide (TBHP) was used to induce oxidative damage, and the antioxidant vitamin E was used as a control for neuroprotective effects. As shown in Figure 5, the oxidative damage induced after 6 h of treatment in the presence of TBHP significantly reduced SH-SY5Y cell viability (50%) compared with the control group ($p < 0.001$). This effect was reduced in the presence of vitamin E, restoring cell survival to 80% ($p < 0.05$). In a similar way, some of the brominated alkaloids protected SH-SY5Y cells against TBHP-induced oxidative damage, avoiding cell death. Compound **5** reduced cellular death at the same level as vitamin E and therefore showed a protective effect at 0.01 and 0.1 μ M ($p < 0.05$, Figure 5). Furthermore, the same effect was observed in the presence of **7** at all concentrations tested ($p < 0.05$, Figure 5). Finally, the most potent activity was observed after treatment with **15**, since neuronal death induced by TBHP was almost totally inhibited, having a stronger neuroprotective effect than vitamin E ($p < 0.05$, Figure 6). Compounds **9**, **11**, **12**, and **18** prevented cell death in a dose-dependent manner, being statistically significant at the highest concentrations tested ($p < 0.05$, Figure 6). Finally, **10** and **13** reduced TBHP-induced cell death at 0.1 and 1 μ M ($p < 0.05$, Figure 5). The rest of the tested compounds did not show any protective effect in SH-SY5Y cells (Figure 5).

To better assess the potential of the nine neuroprotective compounds, their anti-inflammatory activity was tested in activated microglia cells. The activation of microglia leads to the release of pro-inflammatory mediators such as nitric oxide (NO) and the overproduction of these mediators cause oxidative damage in neurons [33]. Therefore, to simulate inflammatory conditions, microglia BV2 cells were activated with lipopolysaccharide (LPS). As shown in Figure 6, when cells were treated with LPS, NO release was doubled compared to control cells ($p < 0.001$). Nevertheless, in the presence of **11** and **15** (0.1 and 1 μ M) or **18** (1 μ M), the NO release was significantly inhibited ($p < 0.01$). Surprisingly, this effect was also observed after incubation in the presence of 0.1 μ M of **9**, **10**, **12**, and **13** but not at 1 μ M. In the same conditions, **5** and **7** did not show any significant activity on the microglia BV2 cells. In both the BV2 and SH-SY5Y cellular models, some brominated alkaloids of this family possess interesting properties in neuroinflammation and neuroprotection.

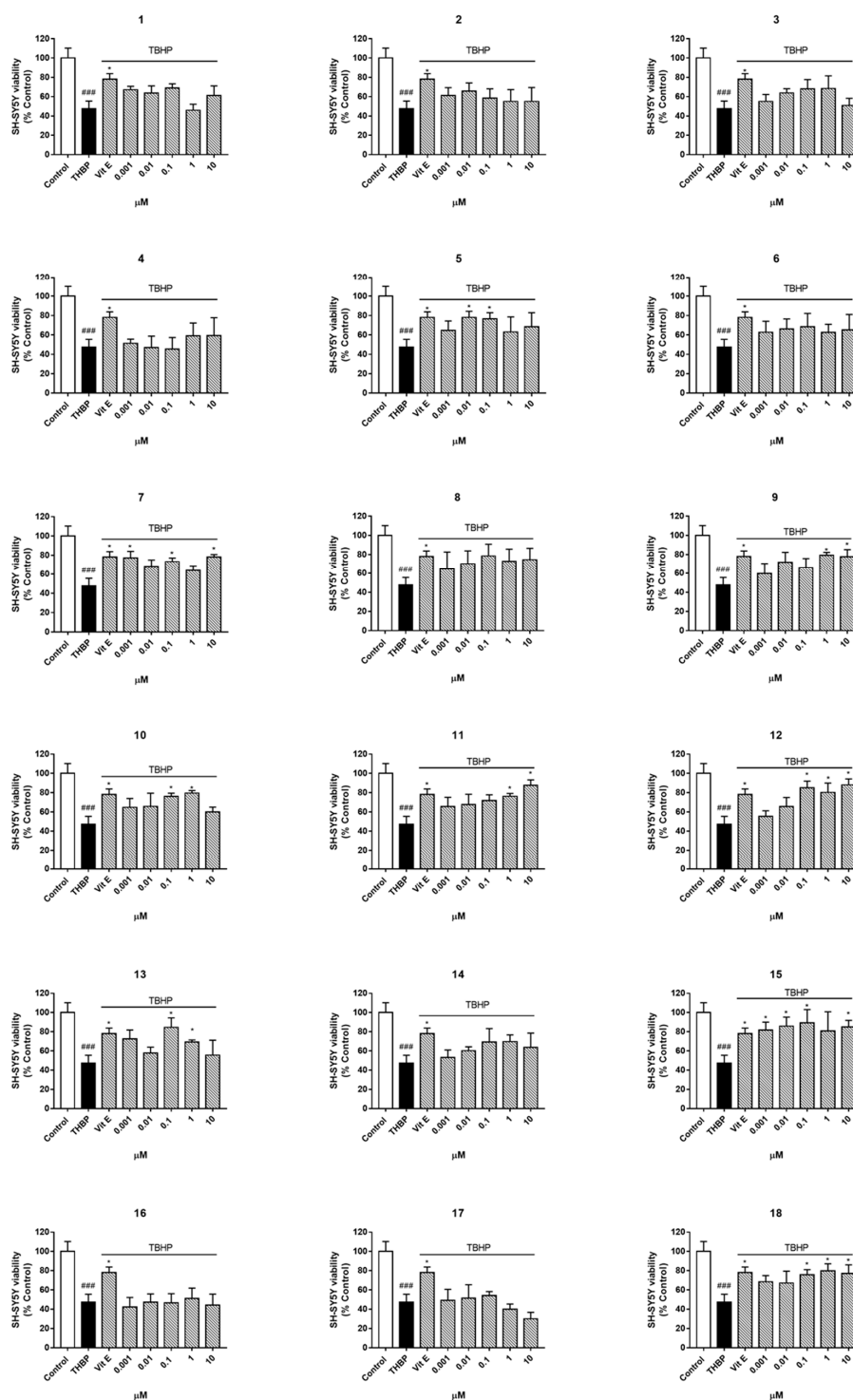


Figure 5. Effect of brominated alkaloids on oxidative damage in neuroblastoma SH-SY5Y cell line. Cells were treated with compounds (0.001, 0.01, 0.1, 1, and 10 μM) in the presence of *tert*-butylhydroperoxide (TBHP) at 65 μM for 6 h. Cell viability was determined using 3-(4,5-dimethylthiazol-2-yl)-2,5-diphenyltetrazolium bromide (MTT) assay. Data are represented in percentage of cell control, being the result of mean absorbance \pm SEM of three independent experiments performed in triplicate. TBHP-treated cells were compared with cells treated with compounds plus TBHP by ANOVA followed by post hoc Dunnett's test. * $p < 0.05$ or TBHP-treated cells versus untreated cells ### $p < 0.001$.

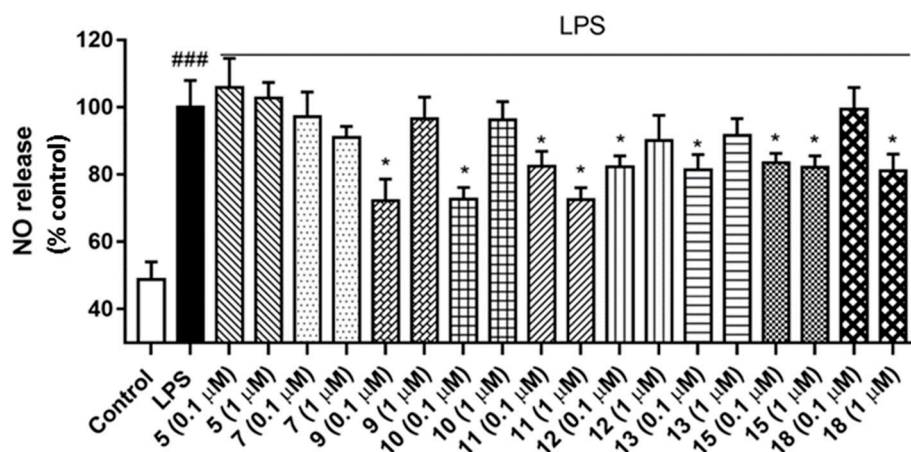
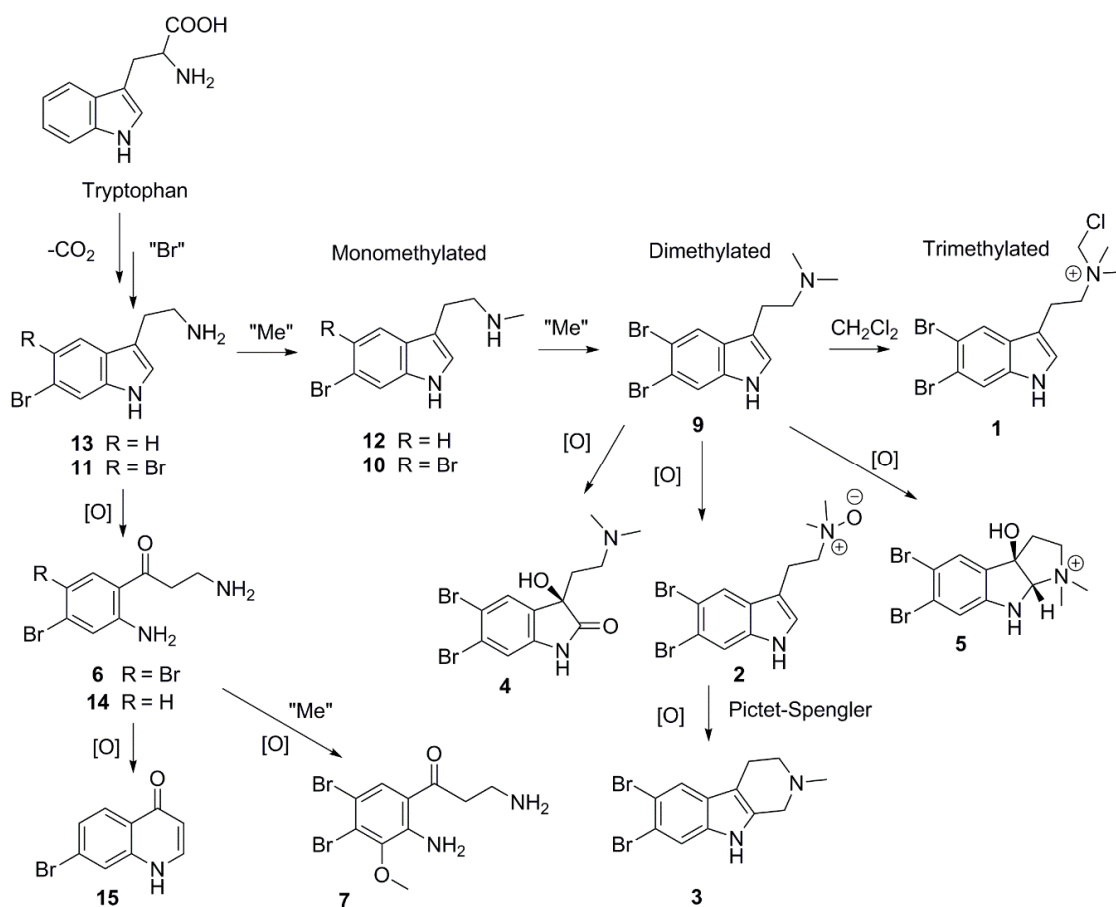


Figure 6. Effects of brominated alkaloids on nitric oxide (NO) release in BV2 microglia cell line. Cells were treated with 5, 7, 9, 10, 11, 12, 13, 15, and 18 at 0.1 and 1 μ M for 1 h before the stimulation with lipopolysaccharide (LPS) at 500 ng/mL for 24 hours. NO release was determined using Griess reagent. Data are represented in percentage of cells treated with LPS, being the result of mean fluorescence intensity \pm SEM of three independent experiments done in duplicate. LPS-treated cells were compared with cells treated with compounds plus LPS by ANOVA followed by post hoc Dunnett's test. * $p < 0.05$ or LPS-treated cells *versus* untreated cells ### $p < 0.001$.

2.3. Biosynthetic Considerations

Both bromotryptamine and bromotyramine families of alkaloids found in the Pacific sponge *Narrabeena nigra* mirror the high potential for marine biodiscovery of sponges found around the Futuna Islands. A microbial origin is likely to be involved in the biosynthesis of these compounds, as analogues of these simple brominated aromatic alkaloids were also found in other groups of invertebrates. Among the five different classes of biogenic metabolites of the bromotryptophan family, the oxindole moiety was indeed reported in the convolutamydines, and the pyrroloindole skeleton in the flustramines, both classes of compounds isolated from bryozoans [34–38]. The β -carboline moiety has already been found in bryozoans [39] and marine sponges from the genus *Hyrtios* [40]. The quinolone 15 was previously described in the sponge *Clathria basilana* and in a bryozoan [41,42], while the kynuramines, as exemplified by 6, were isolated in an undescribed sponge from the Red Sea [22]. Additionally, the known tryptamine derivatives 9–13 have been found in marine invertebrates such as gorgonians [19], tunicates [20], and different sponges of the genera *Ancorina* [43], *Geodia* [21], *Jaspis* [44], *Verongula* [15], *Hyrtios* [14,45], *Aplysina* [46], but mostly in *Smenospongia* [16–18]. The known tyramines 16–18 have been already described in verongioid sponges, [24,47,48] and in an ascidian [23]. Even though both families of compounds were found in *N. nigra*, the majority are bromotryptophan metabolites that are chemotaxonomically related to Dictyoceratida sponges, whereas the bromotyrosine derivatives are associated with the order Verongiida.

Due to the outstanding diversity of bromotryptamine derivatives isolated in this sponge, we postulate simple interconnections among all the isolated metabolites through metabolic transformations that include methylation and different types of oxidation of the indole nucleus (Scheme 1).



Scheme 1. Biosynthetic hypothesis for the formation of the bromotryptophan alkaloids isolated from the sponge *N. nigra*.

To further expand the chemical diversity in this family, the web server Network [49] performing an *in silico* metabolite anticipation was used to assess the presence of minor metabolites involved in this metabolic pathway. As expected, some minor metabolites were identified after comparison of the experimental with calculated MS/MS spectra. These compounds (in orange in Figure 7), which are slightly different from the isolated compounds, could correspond to some biosynthetic intermediates. This is especially true for the formylated compound at m/z 271.0076 resulting from the oxidative cleavage of 6-bromotryptamine (14), which was recently elucidated biosynthetically [50]. Gratifyingly, the cosines of most of the proposed structures are all above 0.5, therefore expressing a high level of confidence (see Supplementary Information) [51]. The proposed structures are also in perfect agreement with the metabolome consistency, using simple and already confirmed biosynthetic transformations [52].

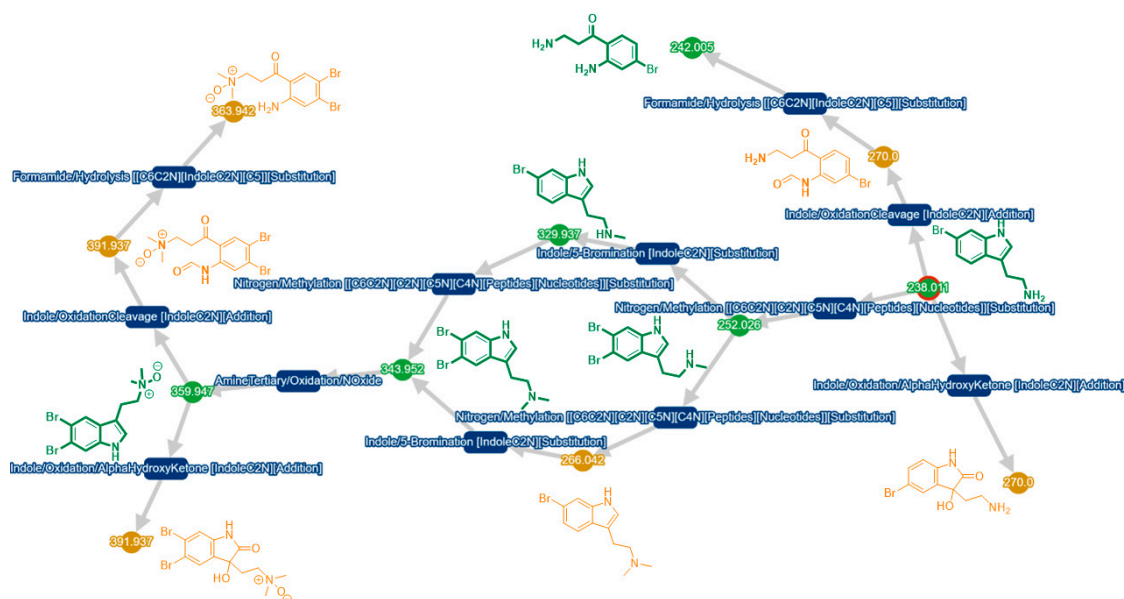


Figure 7. *In silico* metabolization network of the bromotryptamine derivatives present in the fraction of the sponge *N. nigra*. In green are the isolated compounds and in orange, the anticipated structures of minor analogues proposed by the webserver MetWork v0.3.5, Paris [49].

3. Materials and Methods

3.1. General Experimental Procedures

Optical rotation measurements were performed at the Na D line (589.3 nm) with a 5 cm cell at 20 °C on a UniPol L1000 polarimeter (Schmidt + Haensch, Berlin, Germany). UV and ECD data were obtained on Chirascan™ V100 (Applied Photophysics, Leatherhead, UK). NMR experiments were performed on an Inova 500 MHz spectrometer (Varian, Palo Alto, CA, USA) and on a 600 MHz spectrometer (Agilent, Santa Clara, CA, USA). Chemical shifts were referenced in ppm to the residual solvent signals (CD₃OD, at δ_{H} 3.31 and δ_{C} 49.00 ppm; DMSO-*d*₆, at δ_{H} 2.49 and δ_{C} 39.5 ppm). High-resolution mass spectra were obtained with a mass spectrometer UHPLC-HRMS (Agilent 6540, Santa Clara, CA, USA). Purifications were performed using several HPLC-DAD: Jasco (Tokyo, Japan) equipped with PU-2087 pump and UV-2075 detector (preparative), Waters 2690 (Milford, MA, USA) equipped with UV detector 2487 (semipreparative and analytical) and Agilent 1260 (Santa Clara, CA, USA) (analytical).

3.2. Animal Material.

The specimen of *Narrabeena nigra* Kim and Sim 2010 was collected at 8 m depth around the Alofi Island coast (14°20'30" S, 178°04'53" W), in December 2016, during the Tara Pacific expedition. A fragment was fixed with EtOH for taxonomic studies, while the rest of the sample was frozen at −80 °C and freeze-dried for chemical studies. Voucher specimen n° 161213Fu06-01 is stored at NUIG (National University of Ireland, Galway, Ireland).

3.3. Extraction and Purification

The lyophilized and ground sponge (66.8 g) was extracted with MeOH/CH₂Cl₂ at room temperature under sonication (1:1; 3 × 400 mL, 5 min), and the solution was evaporated under reduced pressure. The dried extract (7.27 g) was sequentially fractionated in five fractions by flash silica C-18 VLC with solvents of decreasing polarity: (1) H₂O; (2) H₂O/MeOH (1:1); (3) MeOH; (4) MeOH/CH₂Cl₂ (1:1); and (5) CH₂Cl₂.

Fraction 2 (2.36 g) was purified by repeated semi-preparative reversed phase (RP)-HPLC (Waters SymmetryPrep C18, 7 μm; 7.8 × 300 mm; flow rate: 3.5 mL/min; UV detection: 210 nm), using a

gradient of solvents H₂O:CH₃CN/0.1% TFA (80:20, 5 min; ramp to 70:30 over 20 min; 70:30 for 5 min), which led to 10 peaks (F2P1-F2P10), including **4** ($t_R = 15.8$ min, 1.95 mg, $2.92 \times 10^{-5}\%$ w/w), **9** ($t_R = 24.0$ min, 72.8 mg, $1.09 \times 10^{-3}\%$ w/w) and **16** ($t_R = 17.5$ min, 30.7 mg, $4.60 \times 10^{-4}\%$ w/w). Further purification of F2P1 (Waters XSelect HSS T3, 5 μ m; 4.6×250 mm; flow rate: 1 mL/min; UV detection: 210 nm) with an isocratic solvent composition of H₂O:CH₃CN/0.1% TFA (82:18), led to **17** ($t_R = 18.7$ min, 1.23 mg, $1.84 \times 10^{-5}\%$ w/w) and **18** ($t_R = 14.9$ min, 1.50 mg, $2.25 \times 10^{-5}\%$ w/w). The purification of F2P5 (Waters Xselect Phenyl-hexyl, 5 μ m; 4.6×250 mm; flow rate: 1 mL/min; UV detection: 210 nm) using an isocratic solvent system H₂O:CH₃CN/0.1% TFA (86:14) provided **6** ($t_R = 36.5$ min, 3.92 mg, $5.87 \times 10^{-5}\%$ w/w) and **16** ($t_R = 31.5$ min, 3.25 mg, $4.87 \times 10^{-5}\%$ w/w) and the separation of F2P9 (3.87 mg) (Waters Xselect Phenyl-hexyl, 5 μ m; 4.6×250 mm; flow rate: 1 mL/min; UV detection: 210 nm) with a gradient of solvents H₂O:CH₃CN/0.1% TFA (80:20, 5 min; ramp to 50:50 over 30 min) led to **9** ($t_R = 13.8$ min, 1.50 mg, $2.25 \times 10^{-5}\%$ w/w), **10** ($t_R = 13.2$ min, 1.32 mg, $1.98 \times 10^{-5}\%$ w/w) and **11** ($t_R = 12.5$ min, 0.91 mg, $1.36 \times 10^{-5}\%$ w/w).

Fraction 3 (0.38 g) was purified using the same conditions as those used for fraction 2, and 10 peaks were obtained (F3P1-F3P10), including **2** ($t_R = 29.8$ min, 1.99 mg, $2.98 \times 10^{-5}\%$ w/w), **9** ($t_R = 22.5$ min, 37.2 mg, $5.57 \times 10^{-4}\%$ w/w), and **18** ($t_R = 9.2$ min, 2.48 mg, $3.71 \times 10^{-5}\%$ w/w). Then, the purification of F3P2 (Waters Xselect Phenyl-hexyl, 5 μ m; 4.6×250 mm; flow rate: 1 mL/min; UV detection: 210 nm) was done using an isocratic system of H₂O:CH₃CN/0.1% TFA (87:13) led to **14** ($t_R = 14.4$ min, 0.69 mg, $1.03 \times 10^{-5}\%$ w/w) and **15** ($t_R = 22.9$ min, 1.06 mg, $1.59 \times 10^{-5}\%$ w/w).

The combined F2P4 and F3P4 (6.79 mg) was further purified (Waters Xselect Phenyl-hexyl, 5 μ m; 4.6×250 mm; flow rate: 1 mL/min; UV detection: 210 nm) with H₂O:CH₃CN/0.1% TFA (86:14), which gave **5** ($t_R = 34.0$ min, 1.74 mg, $2.61 \times 10^{-5}\%$ w/w), **12** ($t_R = 31.5$ min, 1.20 mg, $1.80 \times 10^{-5}\%$ w/w), and **13** ($t_R = 26.5$ min, 1.32 mg, $1.98 \times 10^{-5}\%$ w/w). The combined F2P7 and F3P7 (6.02 mg) was further purified (Waters Xselect Phenyl-hexyl, 5 μ m; 4.6×250 mm; flow rate: 1 mL/min; UV detection: 210 nm) with H₂O:CH₃CN/0.1% TFA (82:18), affording **7** ($t_R = 23.9$ min, 2.66 mg, $3.98 \times 10^{-5}\%$ w/w), **8** ($t_R = 19.9$ min, 1.10 mg, $1.65 \times 10^{-5}\%$ w/w), and **16** ($t_R = 17.0$ min, 0.66 mg, $9.88 \times 10^{-6}\%$ w/w).

Fraction 4 (1.03 g) was purified by RP-HPLC (Waters Xselect Prep C18, 5 μ m; 19×250 mm; flow rate: 12 mL/min; UV detection: 210 nm), using an isocratic solvent H₂O:CH₃CN/0.1% TFA (70:30). Further purification of combined F4P6 and F4P7 (10.66 mg) (Waters Xselect Phenyl-hexyl, 5 μ m; 4.6×250 mm; flow rate: 1 mL/min; UV detection: 210 nm) using H₂O:CH₃CN/0.1% TFA (75:25) led to **1** ($t_R = 18.5$ min, 0.92 mg, $1.38 \times 10^{-5}\%$ w/w), **3** ($t_R = 16.0$ min, 2.24 mg, $3.35 \times 10^{-5}\%$ w/w), **9** ($t_R = 13.0$ min, 2.39 mg, $3.58 \times 10^{-5}\%$ w/w), and **10** ($t_R = 11.8$ min, 1.44 mg, $2.16 \times 10^{-5}\%$ w/w).

5,6-Dibromo-N-chloromethyl-N,N-dimethyltryptammonium (**1**)

Yellow amorphous solid; UV (MeOH) λ_{\max} 230, 295 nm; ¹H NMR and ¹³C NMR data, Tables 1 and 2; ESI(+)-HRMS m/z 392.9366 [M]⁺ (calcd. for C₁₃H₁₆Br₂ClN₂, 392.9363, Δ +0.8 ppm).

5,6-Dibromo-N,N-dimethyltryptamine-N-oxide (**2**)

Colorless amorphous solid; UV (MeOH) λ_{\max} 230, 295 nm; ¹H NMR and ¹³C NMR data, Tables 1 and 2; (+)-HRESIMS m/z 360.9557 [M + H]⁺ (calcd. for C₁₂H₁₅Br₂N₂O, 360.9546, Δ +3.0 ppm).

6,7-Dibromo-2-methyltetrahydro- β -carboline (**3**)

Colorless amorphous solid; UV (MeOH) λ_{\max} 231, 290 nm; ¹H NMR and ¹³C NMR data, Tables 1 and 2; (+)-HRESIMS m/z 342.9433 [M + H]⁺ (calcd. for C₁₂H₁₃Br₂N₂, 342.9440, Δ -2.0 ppm).

Narrabeenamine A (**4**)

Yellow amorphous solid; $[\alpha]_D^{20} +12$ (c 0.1, MeOH); UV (CH₃CN) λ_{\max} (log ϵ) 218 (3.66), 260 (3.23), 310 (2.83) nm; ECD (c 2.7×10^{-4} M, CH₃CN) λ_{\max} ($\Delta\epsilon$) 220 (+0.34), 246 (-0.32), 274 (+0.1) nm; ¹H NMR

and ^{13}C NMR data, Tables 1 and 2; (+)-HRESIMS m/z 376.9503 $[\text{M} + \text{H}]^+$ (calcd. for $\text{C}_{12}\text{H}_{15}\text{Br}_2\text{N}_2\text{O}_2$, 376.9495, Δ +2.1 ppm).

Narrabeenamaine B (5)

Yellow amorphous solid; $[\alpha]_{\text{D}}^{20}$ +20 (c 0.1, MeOH); UV (CH₃CN) λ_{max} (log ϵ) 246 (3.52), 310 (2.96) nm; ECD (c 5.5×10^{-4} M, CH₃CN) λ_{max} ($\Delta\epsilon$) 245 (−0.12), 270 (−0.01), 310 (−0.05) nm; ^1H NMR and ^{13}C NMR data, Tables 1 and 2; (+)-HRESIMS m/z 360.9551 $[\text{M}]^+$ (calcd. for $\text{C}_{12}\text{H}_{15}\text{Br}_2\text{N}_2\text{O}$, 360.9546, Δ +1.1 ppm).

5,6-Dibromokynuramine (6)

Yellow amorphous solid; UV (MeOH) λ_{max} 235, 264, 376 nm; ^1H NMR and ^{13}C NMR data, Tables 1 and 2; (+)-HRESIMS m/z 320.9239 $[\text{M} + \text{H}]^+$ (calcd. for $\text{C}_9\text{H}_{11}\text{Br}_2\text{N}_2\text{O}$, 320.9233 Δ +1.9 ppm).

5,6-Dibromo-7-methoxykynuramine (7)

Yellow amorphous solid; UV (MeOH) λ_{max} 240, 265, 377 nm; ^1H NMR and ^{13}C NMR data, Tables 1 and 2; (+)-HRESIMS m/z 350.9344 $[\text{M} + \text{H}]^+$ (calcd. for $\text{C}_{10}\text{H}_{13}\text{Br}_2\text{N}_2\text{O}_2$, 350.9338, Δ +1.7 ppm).

3,5-Dibromo-4-methoxy-N-methyltyramine (8)

Colorless amorphous solid; UV (MeOH) λ_{max} 208, 280 nm; ^1H NMR (500 MHz, CD₃OD) δ_{H} 7.55 (s, H-2 and H-6), 3.85 (s, H-11), 3.24 (t, $J = 7.5$ Hz, H-8), 2.93 (t, $J = 7.5$ Hz, H-7), 2.72 (s, H-10); ^{13}C NMR; (125 MHz, CD₃OD) δ_{C} 154.7 (C, C-4), 136.7 (C-1), 134.3 (C-2, C-6), 119.8 (C-3, C-5), 61.1 (C-11), 50.8 (C-8), 33.7 (C-10), 31.8 (C-7); (+)-HRESIMS m/z 321.9447 $[\text{M} + \text{H}]^+$ (calcd. for $\text{C}_{10}\text{H}_{14}\text{Br}_2\text{NO}$, 321.9437, Δ +3.1 ppm).

3.4. Computational Methods

ECD. The low energy conformers of each compound were generated using the Schrödinger MacroModel 11.3 software package in Maestro release 2017-4 (Schrödinger, LLC, New York, NY, USA) as described previously [53]. The conformers were optimized using Gaussian 16 (Wallingford, CT, USA) at the B3LYP/6-311+G(d,p) level of theory, while at the same time, the zero-point energy, electronic transition, and rotational strength of conformers were calculated for the free-energy distribution of the conformers [54]. The ECD spectrum was calculated using Gaussian 16 at the B3LYP/6-31G(d) level, and spectra were produced using the freely available software SpecDis 1.7 (Berlin, Germany) [55]. All calculations were performed using a polarizable continuum model with acetonitrile. The calculated spectra were then compared to the experimental spectra.

MetWork v0.3.5, Paris, France. Raw MS/MS data were converted into .mgf using MSconvert v3.0.18105-622e002cb, and a molecular network was created using the online workflow at GNPS [51]. The data were filtered by removing all MS/MS peaks within ± 17 Da of the precursor m/z . MS/MS spectra were window filtered by choosing only the top 6 peaks in the ± 50 Da window throughout the spectrum. A network was then created where edges were filtered to have a cosine score above 0.7 and more than 3 matched peaks. Further edges between two nodes were kept in the network if and only if each of the nodes appeared in each other's respective top 10 most similar nodes. The corresponding clustered .mgf was then uploaded to the MetWork server [49]. Compound 13 was used for the in silico metabolization using indole-related biotransformations. For the comparison between experimental and predicted MS/MS spectra, a cosine value threshold of 0.45 was used.

3.5. Bioassays

Cell Culture

Murine microglia BV-2 cell line was purchased from InterLab Cell Line Collection (ICLC, Genoa, Italy), number ATL03001. Cells were maintained in Roswell Park Memorial Institute Medium (RPMI), plus 10% fetal bovine serum (FBS), 100 µg/mL streptomycin and penicillin (100 U/mL) at 37 °C in a humidified atmosphere of 5% CO₂ and 95% air. Cells were dissociated twice a week using 0.05% trypsin/ethylenediaminetetracetic acid (EDTA).

Human neuroblastoma SH-SY5Y cell line was obtained from American Type Culture Collection (ATCC), number CRL2266. Cells were maintained in Dulbecco's Modified Eagle Medium: Nutrient Mix F-12 (DMEN/F-12) plus 10% FBS, 1% glutamax, 100 µg/mL streptomycin and penicillin (100 U/mL) at 37 °C in a humidified atmosphere of 5% CO₂ and 95% air. Cells were dissociated once a week using 0.05% trypsin/EDTA.

Cell Viability

The MTT assay was used to analyze cell viability. Briefly, microglia BV2 cells were cultured in 384 well plates at a density of 2×10^4 cells per well or 2.5×10^4 cells per well in the case of neuroblastoma SH-SY5Y cells. Cells were incubated with different compound concentrations (0.001, 0.01, 0.1, 1, and 10 µM) for 24 h. Then, cells were washed and incubated with MTT [3-(4,5-dimethyl thiazol-2-yl)-2,5-diphenyl tetrazolium bromide] (500 µg/mL) diluted in phosphate buffered saline (PBS) for 1 h at 37 °C. The resulting formazan crystals were dissolved with sodium dodecyl sulfate (SDS), and the absorbance was measured on a spectrophotometer plate reader at 595 nm (Bio-Tek Synergy, Winooski, VT, USA).

Neuroprotection Assay

The neuroprotective effects on cellular viability of compounds in the presence of TBHP were measured by the MTT assay as described above. For this, cells were incubated with compounds at different concentrations (0.001, 0.01, 0.1, 1, and 10 µM) and TBHP (65 µM) for 6 h. The known antioxidant vitamin E (25 µM) was used as a positive control for neuroprotective activity.

NO Determination

The NO concentration in the culture medium was determined using the Griess reagent kit (Thermo Fisher, Madrid, Spain), in accordance with manufacturer's instructions. Briefly, microglia BV2 cells were seeded in 24-well plates (1×10^6 cells per well) and incubated with compounds (1 and 0.1 µM) 1 h before the stimulation with LPS (500 ng/mL) for 24 h. Next, in a 96-well plate it was added 130 µL of deionized water, 150 µL of cells in culture medium, and 20 µL of Griess reagent and then it was incubated for 30 min in the dark and at room temperature. The absorbance was measured on a spectrophotometer plate reader at 548 nm (Bio-Tek Synergy).

4. Conclusions

This work represents the first chemical study of a sponge from the genus *Narrabeena*. The chemical investigation of the Pacific sponge *Narrabeena nigra* collected around the Futuna Islands led to the isolation of a large diversity of simple bromotryptamine and bromotyramine derivatives. As analogues of these families were also found in other marine invertebrates, we hypothesize a microbial origin for these compounds. The use of the webserver MetWork allowed the identification of minor possible biosynthetic intermediates through natural product anticipation based on comparison with calculated MS/MS data.

Overproduction of reactive oxygen species (ROS) generates an oxidative stress state which is related to neurodegenerative diseases. Oxidative stress occurs upon an excessive ROS production

and deficiency of an antioxidant response [56]. Therefore, compounds able to protect neurons against oxidative damage are excellent candidates to be used in neurodegenerative disorders, such as Alzheimer's or Parkinson's disease [57]. In the present work, human neuroblastoma SH-SY5Y cells treated with TBHP for 6 hours were consolidated as a model of oxidative stress damage. Some of the brominated alkaloids, like **5**, showed an interesting neuroprotective effect against TBHP-induced oxidative damage in SH-SY5Y cells, in the same way as the potent antioxidant vitamin E. In addition, seven of these compounds decreased the release of the neurotoxic mediator NO in activated microglia. Activated microglia play a crucial role in neuroinflammation through the excessive production of pro-inflammatory mediators. Further, microglia-mediated inflammation has been related to neurodegenerative diseases [58]. Moreover, these brominated alkaloids showed very low toxicity, up to 10 μ M, in neuron and microglia cell lines. All these results suggest the potential of these natural products as a therapeutic tool to prevent neuronal cell death in age-associated diseases. A recent publication confirms the potential of some oxidized analogues in this series [59]. Nevertheless, further studies will be necessary to better understand the mechanism of action of these compounds.

Supplementary Materials: All NMR, ECD and MS spectra are available online at <http://www.mdpi.com/1660-3397/17/6/319/s1>.

Author Contributions: Conceptualization, A.A., O.P.T., S.G. and M.M.-G.; methodology, J.V., S.G., M.M.-G., A.A. and K.C.; software, G.G.-J. and L.K.J.; validation, J.V., K.C. and A.A.; writing—original draft preparation, M.M.-G.; writing—review and editing, O.P.T. and L.M.B.; supervision, K.C. and A.A.; project administration, O.P.T.; funding acquisition, O.P.T. and L.M.B.

Funding: We are keen to thank the commitment of the people and the following institutions for their financial and scientific support that made this singular expedition possible: CNRS, PSL, CSM, EPHE, Genoscope/CEA, Inserm, Université Cote d'Azur, ANR, agnès b., UNESCO-IOC, the Veolia Environment Foundation, Région Bretagne, Serge Ferrari, Billerudkorsnas, Amerisource Bergen Company, Lorient Agglomération, Oceans by Disney, the Prince Albert II de Monaco Foundation, L'Oréal, Biotherm, France Collectivités, Kankyo Station, Fonds Français pour l'Environnement Mondial (FFEM), Etienne BOURGOIS, the Tara Foundation teams and crew. Tara Pacific would not exist without the continuous support of the participating institutes. Part of this project (Grant-Aid Agreement No. PBA/MB/16/01) is carried out with the support of the Marine Institute and is funded under the Marine Research Program by the Irish Government. M.M.G. acknowledges James Hardiman Research Scholarship (NUI Galway) for supporting her Ph.D. The research leading to the results on bioassays has received funding from the following FEDER co-funded grants: Consellería de Cultura, Educación e Ordenación Universitaria Xunta de Galicia, 2017 GRC GI-1682 (ED431C 2017/01); CDTI and Technological Funds, supported by Ministerio de Economía, Industria y Competitividad, AGL2014-58210-R, AGL2016-78728-R (AEI/FEDER, UE), ISCIII/PI16/01830 and RTC-2016-5507-2, ITC-20161072. From European Union POCTEP 0161-Nanoeaters-1-E-1, Interreg AlertoxNet EAPA-317-2016, Interreg Agritox EAPA-998-2018 and H2020 778069- EMERTOX. S.G. was supported by a fellowship from FIDIS, Spain.

Acknowledgments: We are deeply grateful to The Tara Foundation teams and crew members for their support during the field trip to Futuna. Support and permission to undertake this study were provided by Atoloto Malau (Service de l'environnement, Wallis and Futuna). Roisin Doohan (NUIG) is acknowledged for recording some NMR experiments. We acknowledge the Irish center for high-end computing (ICHEC) for their support and access to the computational resources for DFT calculations.

Conflicts of Interest: The authors declare no conflict of interest. The funders had no role in the design of the study; in the collection, analyses, or interpretation of data; in the writing of the manuscript, or in the decision to publish the results.

References

1. Firsova, D.; Mahajan, N.; Solanki, H.; Morrow, C.; Thomas, O.P. Current Status and Perspectives in Marine Biodiscovery. In *Bioprospecting: Success, Potential and Constraints*; Paterson, R., Lima, N., Eds.; Springer International Publishing AG: Cham, Switzerland, 2017; Volume 16, pp. 29–50.
2. Jaspars, M.; De Pascale, D.; Andersen, J.H.; Reyes, F.; Crawford, A.D.; Ianora, A. The marine biodiscovery pipeline and ocean medicines of tomorrow. *J. Mar. Biol. Assoc. UK* **2016**, *96*, 151–158. [[CrossRef](#)]
3. Snelgrove, P.V.R. An Ocean of Discovery: Biodiversity Beyond the Census of Marine Life. *Planta Med.* **2016**, *82*, 790–799. [[CrossRef](#)]
4. Blunt, J.W.; Carroll, A.R.; Copp, B.R.; Davis, R.A.; Keyzers, R.A.; Prinsep, M.R. Marine natural products. *Nat. Prod. Rep.* **2018**, *35*, 8–53. [[CrossRef](#)] [[PubMed](#)]

5. Bowen, B.W.; Rocha, L.A.; Toonen, R.J.; Karl, S.A. The origins of tropical marine biodiversity. *Trends Ecol. Evol.* **2013**, *28*, 359–366. [[CrossRef](#)] [[PubMed](#)]
6. Tara-Expeditions-Foundation Annual report 2017. Available online: <https://oceans.taraexpeditions.org/en/> (accessed on 25 April 2019).
7. Chancerelle, Y. Coral reefs of Wallis and Futuna: Biological monitoring, health and future. *Rev. Ecol.-Terre Vie* **2008**, *63*, 133–143.
8. Pichon, M. Scleractinia of New Caledonia: Check list of reef dwelling species. In *Compendium of Marine Species from New-Caledonia*, 2nd ed.; Payri, C.E., Richer de Forges, B., Eds.; IRD: Noumea, New-Caledonia, France, 2007; pp. 149–157.
9. Eléonore Vandel, M.P. Pascale Joannot. In *Taxonomic Inventory of Scleractinia in French Overseas Territories, Proceedings of the 12th International Coral Reef Symposium, Cairns, Australia, 9–13 June 2012*; James Cook University: Townsville, Australia.
10. Kim, H.R.; Sim, C.J. A New Species of the Genus *Narrabeena* (Demospongiae: Dictyoceratida: Thorectidae) from Korea. *Korean J. Syst. Zool.* **2010**, *26*, 83–86. [[CrossRef](#)]
11. Prawat, H.; Mahidol, C.; Kawetripob, W.; Wittayalai, S.; Ruchirawat, S. Iodo-sesquiterpene hydroquinone and brominated indole alkaloids from the Thai sponge *Smenospongia* sp. *Tetrahedron* **2012**, *68*, 6881–6886. [[CrossRef](#)]
12. Tasdemir, D.; Bugni Timothy, S.; Mangalindan Gina, C.; Concepción Gisela, P.; Harper Mary, K.; Ireland Chris, M. Cytotoxic Bromoindole Derivatives and Terpenes from the Philippine Marine Sponge *Smenospongia* sp. *Z. Naturforsch. C Biosci.* **2002**, *57*, 914. [[CrossRef](#)]
13. Schoenfeld, R.C.; Conova, S.; Rittschof, D.; Ganem, B. Cytotoxic, antifouling bromotyramines: A synthetic study on simple marine natural products and Their analogues. *Bioorg. Med. Chem. Lett.* **2002**, *12*, 823–825. [[CrossRef](#)]
14. Longeon, A.; Copp, B.R.; Quevrain, E.; Roue, M.; Kientz, B.; Cresteil, T.; Petek, S.; Debitus, C.; Bourguet-Kondracki, M.L. Bioactive Indole Derivatives from the South Pacific Marine Sponges *Rhopaloeides odorabile* and *Hyrtios* sp. *Mar. Drugs* **2011**, *9*, 879–888. [[CrossRef](#)]
15. Kochanowska, A.J.; Rao, K.V.; Childress, S.; El-Alfy, A.; Matsumoto, R.R.; Kelly, M.; Stewart, G.S.; Sufka, K.J.; Hamann, M.T. Secondary Metabolites from Three Florida Sponges with Antidepressant Activity. *J. Nat. Prod.* **2008**, *71*, 186–189. [[CrossRef](#)] [[PubMed](#)]
16. Djura, P.; Stierle, D.B.; Sullivan, B.; Faulkner, D.J. Some Metabolites of the Marine Sponges *Smenospongia aurea* and *Smenospongia (Polyfibrospongia) echina*. *J. Org. Chem.* **1980**, *45*, 1435–1441. [[CrossRef](#)]
17. Tymiak, A.A.; Rinehart, K.L.; Bakus, G.J. Constituents of morphologically similar sponges: *Aplysina* and *Smenospongia* species. *Tetrahedron* **1985**, *41*, 1039–1047. [[CrossRef](#)]
18. Van Lear, G.E.; Morton, G.O.; Fulmor, W. New antibacterial bromoindole metabolites from the marine sponge *Polyfibrospongia maynardii*. *Tetrahedron Lett.* **1973**, *14*, 299–300. [[CrossRef](#)]
19. Pérez, N.; Culioli, G.; Pérez, T.; Briand, J.-F.; Thomas, O.P.; Blache, Y. Antifouling Properties of Simple Indole and Purine Alkaloids from the Mediterranean Gorgonian *Paramuricea clavata*. *J. Nat. Prod.* **2011**, *74*, 2304–2308. [[CrossRef](#)]
20. Fahy, E.; Potts, B.C.M.; Faulkner, D.J.; Smith, K. 6-Bromotryptamine Derivatives from the Gulf of California Tunicate *Didemnum candidum*. *J. Nat. Prod.* **1991**, *54*, 564–569. [[CrossRef](#)]
21. Olsen, E.K.; Hansen, E.; L, W.K.M.; Isaksson, J.; Sepcic, K.; Cergolj, M.; Svenson, J.; Andersen, J.H. Marine AChE inhibitors isolated from *Geodia barretti*: natural compounds and their synthetic analogs. *Org. Biomol. Chem.* **2016**, *14*, 1629–1640. [[CrossRef](#)] [[PubMed](#)]
22. Al Tarabeen, M.; Hassan Aly, A.; Perez Hemphill Catalina, F.; Rasheed, M.; Wray, V.; Proksch, P. New nitrogenous compounds from a Red Sea sponge from the Gulf of Aqaba. *Z. Naturforsch. C Biosci.* **2015**, *70*, 75. [[CrossRef](#)] [[PubMed](#)]
23. Van Wagoner, R.M.; Jompa, J.; Tahir, A.; Ireland, C.M. Trypargine Alkaloids from a Previously Undescribed *Eudistoma* sp. Ascidian. *J. Nat. Prod.* **1999**, *62*, 794–797. [[CrossRef](#)] [[PubMed](#)]
24. Albrizio, S.; Ciminiello, P.; Fattorusso, E.; Magno, S.; Pansini, M. Chemistry of Verongida sponges. I. Constituents of the Caribbean sponge *Pseudoceratina crassa*. *Tetrahedron* **1994**, *50*, 783–788. [[CrossRef](#)]
25. Afoullouss, S.; Calabro, K.; Genta-Jouve, G.; Gegunde, S.; Alfonso, A.; Nesbitt, R.; Morrow, C.; Alonso, E.; Botana, L.M.; Allcock, A.L.; Thomas, O.P. Treasures from the Deep: Characellides as Anti-Inflammatory Lipoglycotriptides from the Sponge *Characella pachastrelloides*. *Org. Lett.* **2019**, *21*, 246–251. [[CrossRef](#)]

26. Buchanan, M.S.; Carroll, A.R.; Pass, D.; Quinn, R.J. NMR spectral assignments of a new chlorotryptamine alkaloid and its analogues from *Acacia confusa*. *Magn. Reson. Chem.* **2007**, *45*, 359–361. [[CrossRef](#)]
27. Capon, R.J. Extracting value: mechanistic insights into the formation of natural product artifacts – case studies in marine natural products. *Nat. Prod. Rep.* **2019**. [[CrossRef](#)]
28. El-Shazly, A.; Wink, M. Tetrahydroisoquinoline and beta-carboline alkaloids from *Haloxylon articulatum* (Cav.) Bunge (Chenopodiaceae). *Z. Naturforsch. C Biosci.* **2003**, *58*, 477–480. [[CrossRef](#)]
29. Cheng, G.-G.; Li, D.; Hou, B.; Li, X.-N.; Liu, L.; Chen, Y.-Y.; Lunga, P.-K.; Khan, A.; Liu, Y.-P.; Zuo, Z.-L.; et al. Melokhanines A–J, Bioactive Monoterpenoid Indole Alkaloids with Diverse Skeletons from *Melodinus khasianus*. *J. Nat. Prod.* **2016**, *79*, 2158–2166. [[CrossRef](#)]
30. Ruiz-Sanchis, P.; Savina, S.A.; Albericio, F.; Álvarez, M. Structure, Bioactivity and Synthesis of Natural Products with Hexahydropyrrolo[2,3-b]indole. *Chem. A Eur. J.* **2011**, *17*, 1388–1408. [[CrossRef](#)]
31. Yan, A.; Liu, Z.; Song, L.; Wang, X.; Zhang, Y.; Wu, N.; Lin, J.; Liu, Y. Idebenone Alleviates Neuroinflammation and Modulates Microglial Polarization in LPS-Stimulated BV2 Cells and MPTP-Induced Parkinson’s Disease Mice. *Front. Cell. Neurosci.* **2018**, *12*, 529. [[CrossRef](#)]
32. Markoutsas, E.; Xu, P. Redox Potential-Sensitive N-Acetyl Cysteine-Prodrug Nanoparticles Inhibit the Activation of Microglia and Improve Neuronal Survival. *Mol Pharm* **2017**, *14*, 1591–1600. [[CrossRef](#)]
33. Colton, C.A. Heterogeneity of microglial activation in the innate immune response in the brain. *J. Neuroimmune Pharmacol.* **2009**, *4*, 399–418. [[CrossRef](#)]
34. Cravotto, G.; Giovenzana, G.B.; Palmisano, G.; Penoni, A.; Pilati, T.; Sisti, M.; Stazi, F. Convolutamidine A: the first authenticated absolute configuration and enantioselective synthesis. *Tetrahedron: Asymmetry* **2006**, *17*, 3070–3074. [[CrossRef](#)]
35. Zhang, H.-P.; Kamano, Y.; Ichihara, Y.; Kizu, H.; Komiyama, K.; Itokawa, H.; Pettit, G.R. Isolation and structure of convolutamydines B ~ D from marine bryozoan *Amathia convoluta*. *Tetrahedron* **1995**, *51*, 5523–5528. [[CrossRef](#)]
36. Carle, J.S.; Christophersen, C. Bromo-substituted physostigmine alkaloids from a marine bryozoa *Flustra foliacea*. *J. Am. Chem. Soc.* **1979**, *101*, 4012–4013. [[CrossRef](#)]
37. Carle, J.S.; Christophersen, C. Marine alkaloids. 2. Bromo alkaloids from a marine bryozoan *Flustra foliacea*. Isolation and structure elucidation. *J. Org. Chem.* **1980**, *45*, 1586–1589. [[CrossRef](#)]
38. Carle, J.S.; Christophersen, C. Marine alkaloids. 3. Bromo-substituted alkaloids from the marine bryozoan *Flustra foliacea*, flustramine C and flustraminol A and B. *J. Org. Chem.* **1981**, *46*, 3440–3443. [[CrossRef](#)]
39. Blackman, A.J.; Matthews, D.J.; Narkowicz, C.K. β -Carboline alkaloids from the marine bryozoan *Costaticella hastata*. *J. Nat. Prod.* **1987**, *50*, 494–496. [[CrossRef](#)]
40. Salmoun, M.; Devijver, C.; Daloze, D.; Braekman, J.-C.; van Soest, R.W.M. 5-Hydroxytryptamine-Derived Alkaloids from Two Marine Sponges of the Genus *Hyrtios*. *J. Nat. Prod.* **2002**, *65*, 1173–1176. [[CrossRef](#)]
41. Mokhlesi, A.; Stuhldreier, F.; Wex, K.W.; Berscheid, A.; Hartmann, R.; Rehberg, N.; Sureechatchaiyan, P.; Chaidir, C.; Kassack, M.U.; Kalscheuer, R.; et al. Cyclic Cystine-Bridged Peptides from the Marine Sponge *Clathria basilana* Induce Apoptosis in Tumor Cells and Depolarize the Bacterial Cytoplasmic Membrane. *J. Nat. Prod.* **2017**, *80*, 2941–2952. [[CrossRef](#)]
42. Tian, X.-R.; Tang, H.-F.; Li, Y.-S.; Lin, H.-W.; Zhang, X.-Y.; Feng, J.-T.; Zhang, X. Studies on the chemical constituents from marine bryozoan *Cryptosula pallasiana*. *Rec. Nat. Prod.* **2015**, *9*, 628–632.
43. Brogan, J.T.; Stoops, S.L.; Crews, B.C.; Marnett, L.J.; Lindsley, C.W. Total Synthesis of (+)-7-Bromotryptargine and Unnatural Analogues: Biological Evaluation Uncovers Activity at CNS Targets of Therapeutic Relevance. *ACS Chem. Neurosci.* **2011**, *2*, 633–639. [[CrossRef](#)]
44. Wang, D.; Feng, Y.; Murtaza, M.; Wood, S.; Mellick, G.; Hooper, J.N.A.; Quinn, R.J. A Grand Challenge: Unbiased Phenotypic Function of Metabolites from *Jaspis splendens* against Parkinson’s Disease. *J. Nat. Prod.* **2016**, *79*, 353–361. [[CrossRef](#)]
45. Aoki, S.; Ye, Y.; Higuchi, K.; Takashima, A.; Tanaka, Y.; Kitagawa, I.; Kobayashi, M. Novel neuronal nitric oxide synthase (nNOS) selective inhibitors, aplysinopsin-type indole alkaloids, from marine sponge *Hyrtios erecta*. *Chem. Pharm. Bull.* **2001**, *49*, 1372–1374. [[CrossRef](#)]
46. Pimentel, S.M.V.; Bojo, Z.P.; Roberto, A.V.D.; Lazaro, J.E.H.; Mangalindan, G.C.; Florentino, L.M.; Lim-Navarro, P.; Tasdemir, D.; Ireland, C.M.; Concepcion, G.P. Platelet Aggregation Inhibitors from Philippine Marine Invertebrate Samples Screened in a New Microplate Assay. *Mar. Biotechnol.* **2003**, *5*, 395–400. [[CrossRef](#)]

47. Ciminiello, P.; Dell'Aversano, C.; Fattorusso, E.; Magno, S.; Pansini, M. Chemistry of Verongida sponges. 10. Secondary metabolite composition of the Caribbean sponge *Verongula gigantea*. *J. Nat. Prod.* **2000**, *63*, 263–266. [[CrossRef](#)]
48. Tian, L.-W.; Feng, Y.; Shimizu, Y.; Pfeifer, T.; Wellington, C.; Hooper, J.N.A.; Quinn, R.J. Aplysinellamides A-C, Bromotyrosine-Derived Metabolites from an Australian *Aplysinella* sp. Marine Sponge. *J. Nat. Prod.* **2014**, *77*, 1210–1214. [[CrossRef](#)]
49. Beauxis, Y.; Genta-Jouve, G. MetWork: A web server for natural products anticipation. *Bioinformatics* **2018**, *35*, 1795–1796. [[CrossRef](#)]
50. Moore, B.S.; Luhavaya, H.; Sigrist, R.; Chekan, J.R.; McKinnie, S.M.K. Biosynthesis of L-4-Chlorokynurenine, a Lipopeptide Antibiotic Non-Proteinogenic Amino Acid and Antidepressant Prodrug. *Angew. Chem. Int. Ed.* **2019**, *58*, 1–7.
51. Wang, M.; Carver, J.J.; Phelan, V.V.; Sanchez, L.M.; Garg, N.; Peng, Y.; Nguyen, D.D.; Watrous, J.; Kapon, C.A.; Luzzatto-Knaan, T.; et al. Sharing and community curation of mass spectrometry data with Global Natural Products Social Molecular Networking. *Nat. Biotechnol.* **2016**, *34*, 828. [[CrossRef](#)]
52. Audoin, C.; Cocandeau, V.; Thomas, P.O.; Bruschini, A.; Holderith, S.; Genta-Jouve, G. Metabolome Consistency: Additional Parazoanthines from the Mediterranean Zoanthid *Parazoanthus Axinellae*. *Metabolites* **2014**, *4*, 421–432. [[CrossRef](#)]
53. Willoughby, P.H.; Jansma, M.J.; Hoye, T.R. A guide to small-molecule structure assignment through computation of (1H and 13C) NMR chemical shifts. *Nat. Prot.* **2014**, *9*, 643. [[CrossRef](#)]
54. Tomasi, J.; Mennucci, B.; Cammi, R. Quantum Mechanical Continuum Solvation Models. *Chem. Rev.* **2005**, *105*, 2999–3094. [[CrossRef](#)]
55. Bruhn, T.; Schaumlöffel, A.; Hemberger, Y.; Bringmann, G. SpecDis: Quantifying the Comparison of Calculated and Experimental Electronic Circular Dichroism Spectra. *Chirality* **2013**, *25*, 243–249. [[CrossRef](#)]
56. Bhattacharya, S.; Gachhui, R.; Sil, P.C. Hepatoprotective properties of kombucha tea against TBHP-induced oxidative stress via suppression of mitochondria dependent apoptosis. *Pathophysiology* **2011**, *18*, 221–234. [[CrossRef](#)]
57. Leirós, M.; Sánchez, J.A.; Alonso, E.; Rateb, M.E.; Houssen, W.E.; Ebel, R.; Jaspars, M.; Alfonso, A.; Botana, L.M. *Spongionella* secondary metabolites protect mitochondrial function in cortical neurons against oxidative stress. *Mar. Drugs* **2014**, *12*, 700–718. [[CrossRef](#)]
58. González-Scarano, F.; Baltuch, G. Microglia as mediators of inflammatory and degenerative diseases. *Annu. Rev. Neurosci.* **1999**, *22*, 219–240. [[CrossRef](#)]
59. Stanley, C.P.; Maghzal, G.J.; Ayer, A.; Talib, J.; Giltrap, A.M.; Shengule, S.; Wolhuter, K.; Wang, Y.; Chadha, P.; Suarna, C.; et al. Singlet molecular oxygen regulates vascular tone and blood pressure in inflammation. *Nature* **2019**, *566*, 548–552. [[CrossRef](#)]

